MODELLING AXIAL MIXING OF CHAR -APPLICATION TO THE DENSE BOTTOM BED IN CFB BOILERS

Anna Köhler*, David Pallarès, Filip Johnsson

Dept. of Energy and Environment
Chalmers University of Technology, SE-412 96 Göteborg, Sweden

Email: anna.koehler@chalmers.se*

Abstract – This work presents a semi-empirical two-phase model for the axial mixing of a spherical tracer particle, aiming to represent a char particle, with application to conditions relevant for the dense bottom bed flow in CFB boilers. The velocity fields of both the bubble and emulsion phases are modelled with validated expressions from literature, while the velocity of the tracer particle in the emulsion phase is obtained from the equation of motion. A correlation for the drag force created by the bed and acting on the tracer particle is found with the help of experimental data from fluid-dynamically down-scaled tests (Köhler et al, 2017). The model is used to predict trends in axial mixing with operational parameters (fluidization velocity, dense bed height) and tracer properties (size and density), which agree well with experimental findings in literature.

NOTATION

a, b	Constants, Eq. (15)	K	Material constant
A_o	Bubble catchment area, m^2	m_p	Mass of fuel particle, kg
a_p	Acceleration of fuel particle, m/s^2	q	Probability to start rising, %
C_d	Drag coefficient	u_b	Bubble flow velocity, m/s
D_b	Bubble diameter, m	u_{br}	Single bubble velocity, m/s
d_m	Bed material particle diameter, mm	u_{mf}	Minimum fluidisation velocity, m/s
D_p	Tracer particle diameter, m	u_o	Fluidization velocity, m/s
f	Function, Eq (9)	u_s	Velocity of sinking solids, m/s
F_{add}	Added mass force, N	u_{tr}	Throughflow velocity, m/s
F_b	Buoyancy force, N	u_{vis}	Visible bubble flow velocity, m/s
F_d	Drag force, N	z	Height in the bed, m
F_g	Gravitational force, N	α	Fuel particle to bubble velocity
f_w	Bubble wake fraction	δ	Bubble fraction
g	Gravitational constant, m/s^2	ρ	Density, kg/m^3
H_o	Fixed bed height, m		

INTRODUCTION

Fluidised bed (FB) units have been used commercially for combustion and gasification of solid fuels since the early 1970s (Koornneef et al., 2007). There are mainly two types of FBs used in fuel conversion applications: bubbling fluidised beds (BFB) and circulating fluidised beds (CFB). While the basic concept is the same as for BFBs, CFB units are operated at higher fluidization velocities, causing a significant share of the bed material in the lower part of the furnace to be entrained into the freeboard of which a certain share is entrained out of the riser (furnace). The particles leaving the furnace have to be recirculated back into the riser. CFB reactors are common for large installations up to several hundreds of MWe, where higher investment costs are compensated with higher temperatures and efficiencies, whereas BFB reactors are preferably used for installation of lower capacity using low quality fuels, such as waste and biomass with high moisture content and low heating values used in CHP schemes in district heating systems. In the lower part of a CFB furnace, there is a dense bed region, which has been shown to be similar to that of BFB units (see e.g. Svensson et al. (1996)). As the initially packed bed solids are fluidised beyond the minimum fluidisation velocity (which, for Geldart B particles coincides with the minimum bubbling velocity), bubbles are formed at the bottom and start travelling upwards through the dense bed. The dense bottom bed bubble flow is obviously a key mechanism for mixing of the bed material and fuel particles and thus, influences the conversion of the latter.

The axial mixing of the fuel particles has a strong impact on the fuel conversion rate, as both the heat and mass transfer with the surrounding is influenced as the fuel particles are moving within and above the bed. At the dense bed surface, the presence of less bulk particles surrounding the fuel particles yields an enhancement of

the bed-to-fuel mass transfer and a decrease in the bed-to-fuel heat transfer, compared to an immersed fuel particle (Lundberg et al., 2016). Compared to immersed fuel particles, particles "floating" on the dense bed surface experience a faster lateral mixing, which is an important parameter influencing the design of the furnace. As FB units handle a large variety of solid fuels (e.g. coal, biomass, peat, waste), the fuel density and size can range widely, giving rise to different lateral as well as axial fuel mixing behaviours under given operational conditions.

Modelling combined with experimental work are key tools for the understanding of fuel mixing properties under various FB conditions with the aim to obtain design tools for development and reliable scale-up of FB units. A challenge is the complexity as the mixing is governed by multiphase flow with significant exchanges of mass, momentum and heat in presence of chemical reactions. There are two main types of modelling for large-scale FBs: semi-empirical modelling (in which velocity fields of the gas and bulk solids are not solved by momentum balances but by simpler models and assumptions) and computational fluid dynamics (CFD, in which transport equations for mass, momentum and heat are solved). Semi-empirical process models usually lack in detail as they use many simplified assumptions, but can simulate the whole process at affordable computational costs (hours), which makes them a powerful tool for design and engineering purposes (Ratschow, 2009, Pallarès and Johnsson, 2008, Myöhänen and Hyppänen, 2011), but obviously relying on their underlying assumptions. CFD provides results on the momentum transfer and has better spatial resolution but still presents uncertainty in simulation results, mainly due to the difficulty in resolving the solids flow structures at sub-grid level and CFD is computationally costly (weeks/months).

The aim of this work is to develop a first version of a semi-empirical two-phase model to describe the axial mixing of a large spherical particle, mimicking a char particle, within the dense bed. Different correlations available in literature are investigated and used to describe the bubble and emulsion flow in the bed. To describe the motion of the tracer particle in the emulsion phase, the equation of motion of the particle is solved. The model uses experimental data by Köhler et al. (2017), sampled in a 3-dimensional fluid-dynamically down-scaled bubbling fluidized bed by means of magnetic particle tracking (MPT), in order to describe the drag force from the bed solids acting on the tracer particle. The aim is to implement the model together with a model for the mixing in lateral direction as part of a comprehensive model for large-scale fuel conversion in circulating fluidized beds (Pallarès and Johnsson, 2008). Yet, more work is required to develop these models before they can be implemented in the comprehensive model.

THEORY

In this work the dense bed is divided into two phases: the emulsion phase and the bubble phase. The emulsion phase contains all bulk solids at minimum fluidisation velocity, while the bubble phase is a fluid phase with only a small amount of the total solids present in the bubble wakes. Fig. 1 gives a schematic of the two-phase model including variables and their equations. The tracer particle is allowed to flow within each of the two phases and change phase. As motion and mixing of the bed material is assumed to be solely driven by the rise of bubbles through the bed, bubble flow characteristics become crucial to determine the velocities of the emulsion phase.

Modelling of the bubble phase

The bubble rising velocity of a single bubble released in a liquid was originally described theoretically by Davies and Taylor (1950) using the radius of the curvature of the bubble. Davidson and Harrison (1963) compared different empirical expressions for a single bubble in a bed at minimum fluidisation and an equation they present, which is commonly used in literature until today, is defined as

$$u_{br} = 0.711 \cdot \sqrt{g \cdot D_b} \tag{1}$$

where D_b is the equivalent diameter of a sphere with the same volume as the spherical cap bubble. Rowe and Patridge (1965) later correlated the equation to different bed materials of various particle sizes and densities and defined

$$u_{br} = 0.25\, K \cdot \sqrt{g \cdot D_b} \tag{2}$$

where K is a constant dependent on the properties of the bed material. Rowe and Patridge (1965) originally used the bubble radius, however, in this work the equation is expressed with the bubble diameter, wherefore K is multiplied with a factor of 0.25. Eq. (2) is used in the present work as this form is more flexible than Eq. (1) and allows for different values of K. There are many different definitions for the bubble size in literature

(Rowe, 1976, Darton et al., 1977, Kunii and Levenspiel, 1991, Baeyens and Wu, 1992). For this model the bubble diameter was taken from a correlation by Darton et al. (1977), which is more suitable for freely bubbling beds as it takes into account the growth by coalescence with other bubbles, which was found to correlate well with experimental data from other authors (Johnsson et al., 1991). Keeping the constant *K*, Eq. (2) becomes

$$u_{br} = 0.809 g^{0.4} (0.25K)^{0.8} \cdot \left(u_o - u_{mf}\right)^{0.2} \cdot \left(z + 2.64\sqrt{A_0}\right)^{0.4} \quad (3)$$

where z is the height of the bubble and A_o is the bubble catchment area.

When releasing a single bubble into a bed at minimum fluidisation velocity, it rises with the velocity u_{br}. The bubble velocity in bubbling beds is then described by superimposing the rise velocity of the single bubble with the excess gas velocity used to fluidise the bed (Davidson and Harrison, 1963). Taken into account that it has been shown that there is a throughflow in and between bubbles, which makes bubble expansion less than if the flow would have been expressed by the original two-phase flow theory, the bubble velocity is written (*cf.* Johnsson et al. (1991) and references therein)

$$u_b = u_o - u_{mf} - u_{tr} + u_{br} \quad (4)$$

where u_o is the superficial gas velocity, u_{mf} is the minimum fluidisation velocity and u_{tr} is the velocity of the throughflow. The throughflow was originally introduced for bubbling beds with high fluidisation velocity. However, Johnsson et al. (1991) and Pallarès and Johnsson (2006) concluded that its influence is of relevance also at relatively low velocities when applying Group B solids as is typically used in FB boilers.

The total gas flow into the bed is the sum of the flow through the emulsion phase, u_{mf}, the visible bubble flow, u_{vis}, and the throughflow, u_{tr} (Fig. 1). The volume fraction of the bubble phase is defined by the bubble density, δ, so that the visible bubble flow can be expressed as $u_{vis} = \delta\, u_b$ and the total gas flow becomes

$$u_o = u_{mf} + u_{vis} + u_{tf} = u_{mf} + \delta u_b + u_{tf} \quad (5)$$

With Eqs. (4) and (5) the bubble density becomes

$$\delta = \frac{1}{1 + \frac{u_{br}}{u_o - u_{mf} - u_{tf}}} \quad (6)$$

The bubble density is independent of the height of the bubbles in the bed. This is as the pressure drop inside the dense bed is constant with height and therefore also the bed porosity, i.e. the bubble density is constant. With this, according to Johnsson et al. (1991), an expression for the throughflow as correction factor is obtained

$$u_{tf} = \left(1 - f\left(z + 2.64\sqrt{A_o}\right)^{0.4}\right)\left(u_o - u_{mf}\right) \quad (7)$$

With Eq. (7) in (6) the bubble density becomes

$$\delta = \frac{1}{1 + \frac{0.809(0.25K)^{0.8} g^{0.4}}{f}\left(u_o - u_{mf}\right)^{-0.8}} \quad (8)$$

where f_2 is an empirical expression taken from experiments in a hot unit (Johnsson et al., 1991) to be

$$f = [0.26 + 0.70\, exp(-3.3 d_m)] \times \left[0.15 + \left(u_o - u_{mf}\right)\right]^{-0.33} \quad (9)$$

where d_m is the particle diameter of the bed material in mm.

Within the bubble phase the velocity of the fuel particle is expressed in relation to the bubble velocity.

$$u_p = \alpha \cdot u_b \quad (10)$$

Eq. (10) is taking into account that the particle slides along a bubble or its wake, thus, might not been dragged up from one bubble solely. Works in literature has estimated the velocity of large objects to range from 10% and 30% of the bubble velocity (Nienow et al., 1978, Rios et al., 1986, Lim and Agarwal, 1994, Rees et al., 2005, Soria-Verdugo et al., 2011). The present work applies $\alpha = 0.15$, yielded reasonable results of the tracer particle velocity.

Modelling of the dense phase

While bulk solids are dragged upwards in the wakes of the rising bubbles, they sink in the emulsion phase in order to keep the mass balance. From a simple mass balance over the two phases the velocity of the sinking particles is expressed as

$$u_s = \frac{f_w \cdot \delta \cdot u_b}{(1 - \delta - f_w \delta)} \quad (11)$$

where f_w is the wake volume fraction of the rising bubbles. Note that this expression excludes particles in the bubble wakes ($f_w\ \delta$) from the emulsion phase (Kunii and Levenspiel, 1991). Values for the wake fraction are available from experiments using Geldart B particles of various sizes and densities (Rowe and Partridge, 1965). Fig. 2 shows the development of the bubble velocity, u_b, and the sinking solids velocity, $|u_s|$, over bed height.

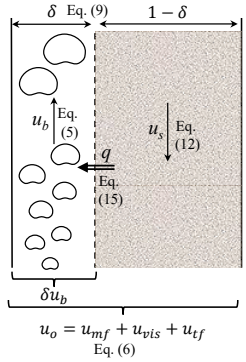

Fig. 1: Schematic of two phase model.

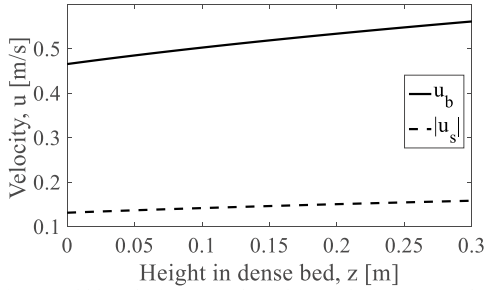

Fig. 2: Bubble velocity, u_b, and emulsion velocity, u_s, over bed height z.

The motion of a fuel particle in the emulsion phase is defined by the sum of forces acting on the tracer particle: the gravitational force, the buoyancy force, the drag force and the added mass force

$$m_p a_p = F_g + F_b + F_d + F_{add} \tag{12}$$

which can be re-written as

$$a_p = \left(\frac{\rho_s}{\rho_p} - 1\right) \cdot g + \frac{3}{4}\frac{\rho_s}{\rho_p}\frac{C_d}{D_p}\left|(u_s - u_p)\right| \cdot (u_s - u_p) + \frac{\rho_s}{2\rho_p}\left(\frac{Du_s}{Dt} - \frac{du_p}{dt}\right) \tag{13}$$

The added mass force, i.e. the force to accelerate the mass of fluid around the particle (Clift et al., 1978), can in more detail be expressed as the following

$$F_{ad} = \frac{\rho_s}{2\rho_p}\left(\frac{Du_s}{Dt} - \frac{du_p}{dt}\right) = \frac{\rho_s}{2\rho_p}\left(\frac{du_s}{dt} + u_p\frac{du_s}{dz} - \frac{du_p}{dt}\right) \tag{14}$$

In Eq. (14) the velocity field of the solid phase is considered constant over time. Values for the height derivative of the emulsion solids velocity are taken from the data in the dashed curve in Fig. 2 (note that they are rather small).

Drag force acting on tracer particle

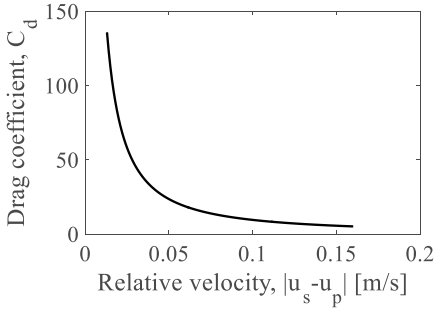

Fig. 3: Drag coefficient, C_d, as function of relative particle velocity, u_p-u_s.

The drag coefficient acting on the tracer particle is unknown and has to be evaluated with help of experimental data to be able to model the motion of the tracer particle. To do this, minimum and maximum acceleration values of the tracer particle are taken from MPT measurements previously obtained by the authors (Köhler et al., 2017) and inserted for a_p in Eq. (13). Since the gravitational and buoyancy force terms are known, with the extreme values for $a_p = du_p/dt$ the added mass force can be determined by assuming the relative particle velocity to vary between the solid phase velocity, u_s, and $0.1u_s$. This is assuming that the actual particle velocity vary between zero and 90% of the solids phase velocity. With this, values for the drag coefficient can be determined from Eq. (13).

The values of a_p are used to fit a drag coefficient function of the relative particle velocity according to the form:

$$C_d = \frac{a}{(u_s - u_p)^b} \quad \text{with} \quad a = 0.48,\ b = 1.3 \tag{15}$$

Fig. 3 shows the resulting estimated drag coefficient curve for the fuel particle in the emulsion phase. Note, in this current version of the model the drag coefficient is not dependent on the tracer diameter, which constitutes a limitation (as discussed later in connection to Fig. 8).

Transfer between emulsion and bubble phase

When sinking in the particulate phase, the fuel particle may leave the sinking state in the emulsion phase by being transferred to the bubble phase where it starts rising again until it reaches the dense bed surface, where it re-joins the emulsion phase. This phase change is here considered to occur with a probability, q, which for the first approximation used in this work is assumed constant along the entire height of the bed. For the time step used of 0.02 s the interphase net transfer probability is set to:

$$q = 0.03 \tag{16}$$

It should be noted that even if in reality fuel can also to a limited extent be transferred from the bubble phase to the emulsion phase, the current model considers only the net transfer from the emulsion to the bubble phase.

Time marching

The fuel velocity and the location in each phase as well as the fuel interphase transfer can be calculated in a dynamic simulation by solving stepwise Eqs. (10) and (13), and after every time step in the emulsion phase Eq. (16) gives if the tracer particle is transferred to the bubble phase. The dynamic simulation is run until enough robust statistics are reached (typically 900 s of simulated time). Fig. 4 exemplifies the transient vertical location of a tracer particle over 30 seconds of simulation time. Table 1 gives an overview of the model inputs used for this simulation.

Table 1: Model inputs

Parameter	Hot model
Temperature	800 °C
Bed material density	2 600 kg/m^3
Bed material size	250 µm
Bed height	$H_0 = 0.3\ m$
Tracer diameter	$D_p = 0.05\ m$
Tracer density	$\rho_p = 1230 \frac{kg}{m^3}$
Ratio u_s to u_b	$\alpha = 0.15$
Probability to start rising	$q = 0.03$
Time step	0.02 s
Total modelling time	900 s

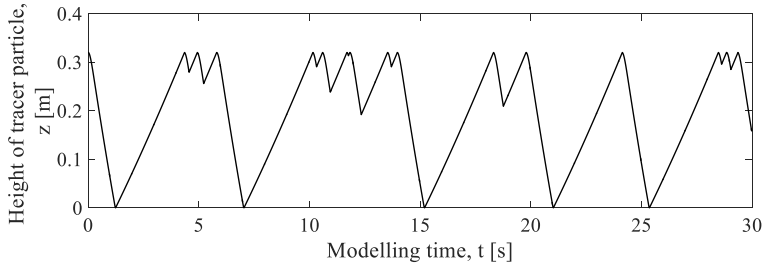

Fig. 4: Axial location of the tracer over 30 seconds of modelling time.

RESULTS AND DISCUSSION

Fig. 5 shows the probability density function (PDF) of the vertical location of the fuel tracer, z, comparing the modelling results with measurement data obtained from MPT (from Köhler et al. (2017)) for a fluidisation velocity of 0.19 m/s and a fixed bed height of 0.3 m. The expansion of the bed height due to fluidisation is taken into account in the model, yielding a dense bed height of 0.32 m. The current scope of the model does not include the splash zone above the dense bed, while MPT obviously does. In the dense bed the model follows well the trend of the measured data. The tracer probability peaks at the dense bed surface and declines towards the bottom of the bed.

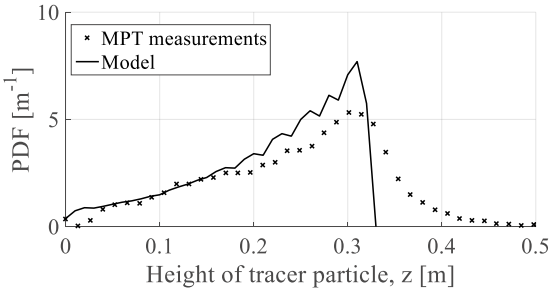

Fig. 5: Comparison of modelling results with MPT data (Köhler et al., 2017) using vertical position of the tracer.
$u_o - u_{mf}$ = 0.19 m/s, H_o = 0.3 m,. D_p = 0.04 m, ρ_p = 1230 kg/m³

Fig. 6 shows the distribution of axial location of the tracer, z, for a fixed bed height of 0.3 m. The graph compares different fluidisation velocities: 0.19, 0.37 and 0.55 m/s. It can be seen that an increase in fluidisation velocity yields a more evenly mixing of the tracer in the dense bed, which is in line with experimental results (Rowe et al., 1972, Nienow et al., 1978, Fotovat et al., 2015, Köhler et al., 2017). Note that increasing the fluidization velocity beyond 0.37 m/s hardly yields any variation in the axial distribution of the fuel, i.e. indicating that the particle is already well mixed into the bed.

In Fig. 7 the fuel tracer distributions are plotted for a fixed fluidisation velocities of 0.19 m/s, comparing three different fixed bed heights: 0.2, 0.3 and 0.4 m. It can be concluded that a change in bed height has a similar effect on the tracer distribution in the dense bed as increasing the fluidisation velocity. As derived from Eq. (3), with increasing height in the bed, the bubbles grow bigger and rise faster, which improves mixing in the bed, i.e. the maxima of the distribution of the axial tracer position decrease for higher beds (Davidson and Harrison, 1963).

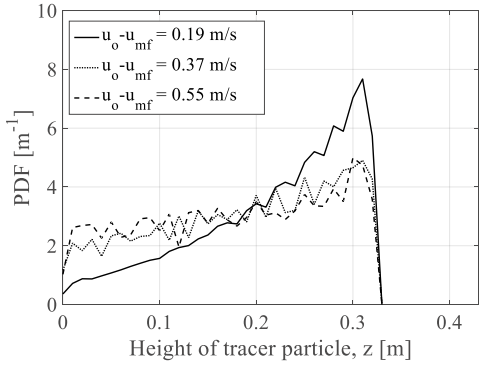

Fig. 6: Modelled results of the axial distribution of the fuel tracer at different fluidisation velocities. *H_o = 0.3 m, D_p = 0.04 m, ρ_p = 1230 kg/m³.*

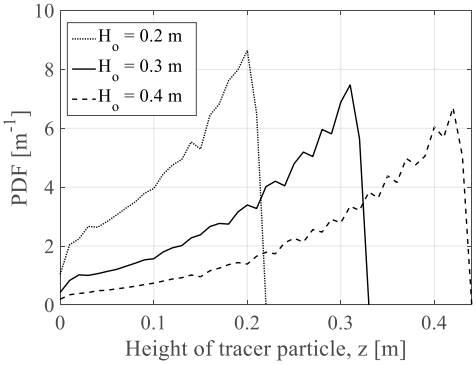

Fig. 7: Modelled results of the axial distribution of the fuel tracer at different fixed bed heights.
u_o - u_{mf} = 0.19 m/s, D_p = 0.04 m, ρ_p = 1230 kg/m³.

Fig. 8 shows the axial distribution of the fuel tracer for a fixed bed height of 0.3 m and a fluidisation velocity of 0.19m/s, comparing different tracer sizes for a tracer density of 1230 kg/m³. With increasing tracer particle diameter the fuel particle mixes less into the dense bed. This is as the buoyancy force grows faster with tracer particle size ($F_b = f(D_p^3)$) than the drag force ($F_d = f(D_p^2)$), increasing the relative influence of the buoyancy effect, Eq. (13). (Note, that extreme values for D_p are shown here. In this case this is rather to test the limitation of the model than mimic real fuel particles.)

Fig. 9 gives model simulations with a fixed bed height of 0.3 m and a fluidisation velocity of 0.37 m/s comparing different tracer densities (800, 900 and 1230 kg/m³). With decreasing particle density the particle becomes more buoyant (Eq. (13)) and mixes less into the bed, which is expected and in line with trends found experimentally (Köhler et al., 2017). However, the lightest tracer (800 kg/m³), which corresponds to the

density of biomass, shows here a rather flotsam behaviour, while in the experiments the tracer with the same density was mixed well into the bed at a fluidisation velocity of 0.37 m/s.

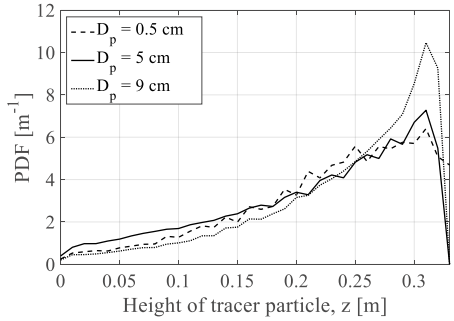

Fig. 8: Modelling results of vertical position of the tracer, comparing different particle diameters for H_o =0.3 m, $u_o - u_{mf}$ = 0.19 m/s, ρ_p = 1230 kg/m^3.

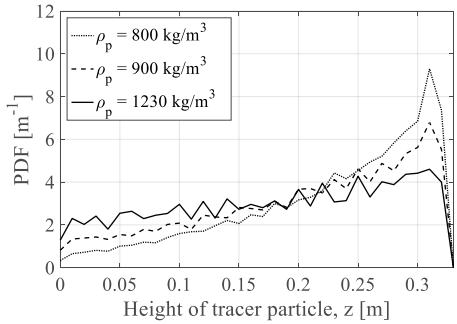

Fig. 9: Modelling results of vertical position of the tracer, comparing different particle densities for H_o = 0.3 m, $u_o - u_{mf}$ = 0.37 m/s, D_p = 0.05 m.

In all, it is concluded that the above presented modelling results seem promising and that the modelling concept should be developed further. Thus, a further developed version of this model will also account for the probability of the rising tracer particle to be entrained into the emulsion phase and start sinking instead of assuming that the particle rises all the way to the bed surface once it is entrained into to the bubble phase. The probability to start sinking as well as the probability to start rising, i.e. changing from one phase to the other, are to be dependent on the bed height. This is since the bubble size and velocity varies with height. Further the tracer motion in the splash zone will be included, as well as the dependency of the drag coefficient on the particle diameter. The model will be combined with a model for the mixing in the lateral direction. When validated, the model will be integrated into a comprehensive model for fuel conversion in large-scale circulating fluidized beds (Pallarès and Johnsson, 2008).

CONCLUSIONS

A first version of a semi-empirical two-phase model for modelling axial mixing of a spherical tracer particle mimicking fuel mixing in a dense bed region of a fluidised bed boiler is developed. The model describes the bubble and emulsion phase with correlations available in literature and simulates the velocity of the tracer particle in the emulsion phase by solving its equation of motion. Therefore, a correlation for the drag force on the fuel particle is developed:

$$C_d = \frac{a}{(u_s - u_p)^b} \quad \text{with} \quad a = 0.48,\ b = 1.3$$

The model is implemented and the modelling results are compared with experimental data from measurements in a fluid-dynamically down-scaled BFB by means of magnetic particle tracking (Köhler et al., 2017). The model results show that, for typical fuel properties (larger and lighter than the bulk solids), the axial mixing of fuel increases with fluidisation velocity, dense bed height, reduced fuel size and increased particle density. This is well in line with experimental findings from literature.

REFERENCES

BAEYENS, J. & WU, S. Y. 1992. Bed expansion and the visible bubble flow rate in gas fluidized beds. *Advanced Powder Technology,* 3**,** 163-189.

CLIFT, R., GRACE, J. R. & WEBER, M. E. 1978. *Bubbles, Drops and Particles,* New York, Academic Press

DARTON, R. C., LA NAUZE, R. D., DAVIDSON, J. F. & HARRISON, D. 1977. Bubble Growth Due To Coalescence in Fluidized Beds. *Transactions of the Institution of Chemical Engineers,* 55**,** 274-280.

DAVIDSON, J. F. & HARRISON, D. 1963. Fluidised particles New York Cambridge University Press

DAVIES, R. M. & TAYLOR, G. 1950. The Mechanics of Large Bubbles Rising through Extended Liquids and through Liquids in Tubes. *Proceedings of the Royal Society of London. Series A. Mathematical and Physical Sciences,* 200**,** 375-390.

FOTOVAT, F., ANSART, R., HEMATI, M., SIMONIN, O. & CHAOUKI, J. 2015. Sand-assisted fluidization of large cylindrical and spherical biomass particles: Experiments and simulation. *Chemical Engineering Science,* 126**,** 543-559.

JOHNSSON, F., ANDERSSON, S. & LECKNER, B. 1991. Expansion of a freely bubbling fluidized bed. *Powder Technology,* 68**,** 117-123.

KOORNNEEF, J., JUNGINGER, M. & FAAIJ, A. 2007. Development of fluidized bed combustion—An overview of trends, performance and cost. *Progress in Energy and Combustion Science,* 33**,** 19-55.

KUNII, D. & LEVENSPIEL, O. 1991. *Fluidization Engineering*, Butterworth-Heinemann.

KÖHLER, A., RASCH, A., PALLARÈS, D. & JOHNSSON, F. 2017. Experimental characterization of axial fuel mixing in fluidized beds by magnetic particle tracking. *Powder Technology, http://dx.doi.org/10.1016/j.powtec.2016.12.093*.

LIM, K. S. & AGARWAL, P. K. 1994. Circulatory motion of a large and lighter sphere in a bubbling fluidized bed of smaller and heavier particles. *Chemical Engineering Science,* 49**,** 421-424.

LUNDBERG, L., TCHOFFOR, P. A., PALLARÈS, D., JOHANSSON, R., THUNMAN, H. & DAVIDSSON, K. 2016. Influence of surrounding conditions and fuel size on the gasification rate of biomass char in a fluidized bed. *Fuel Processing Technology,* 144**,** 323-333.

MYÖHÄNEN, K. & HYPPÄNEN, T. 2011. A Three-Dimensional Model Frame for Modelling Combustion and Gasification in Circulating Fluidized Bed Furnaces. *International Journal of Chemical Reactor Engineering.*

NIENOW, A. W., ROWE, P. N. & CHIWA, T. 1978. Mixing and segregation of a small proportion of large particles in gas fluidized beds of considerably. *AIChE Symposium Series,* 74**,** 45-53.

PALLARÈS, D. & JOHNSSON, F. 2006. Macroscopic modelling of fluid dynamics in large-scale circulating fluidized beds. *Progress in Energy and Combustion Science,* 32**,** 539-569.

PALLARÈS, D. & JOHNSSON, F. 2008. Modeling of fuel mixing in fluidized bed combustors. *Chemical Engineering Science,* 63**,** 5663-5671.

RATSCHOW, L. 2009. *Three-Dimensional Simulation of Temperature Distributions in Large-Scale Circulating Fluidized Bed Combustors.* Hamburg University of Technology

REES, A. C., DAVIDSON, J. F., DENNIS, J. S. & HAYHURST, A. N. 2005. The rise of a buoyant sphere in a gas-fluidized bed. *Chemical Engineering Science,* 60**,** 1143-1153.

RIOS, G. M., DANG TRAN, K. & MASSON, H. 1986. FREE OBJECT MOTION IN A GAS FLUIDIZED BED. *Chemical Engineering Communications,* 47**,** 247-272.

ROWE, P. N. 1976. Prediction of bubble size in a gas fluidised bed. *Chemical Engineering Science,* 31**,** 285-288.

ROWE, P. N., NIENOW, A. W. & AGBIM, A. J. 1972. The mechanisms by which particles segregate in gas fluidised beds - binary systems of near-spherical particles *Transactions of the Institution of Chemical Engineers* 50**,** 310-323.

ROWE, P. N. & PARTRIDGE, B. A. 1965. An X-ray study of bubbles in fluidised beds. *Trans. Instn. Chem. Engrs.,* 43**,** 157-175.

SORIA-VERDUGO, A., GARCIA-GUTIERREZ, L. M., GARCÍA-HERNANDO, N. & RUIZ-RIVAS, U. 2011. Buoyancy effects on objects moving in a bubbling fluidized bed. *Chemical Engineering Science,* 66**,** 2833-2841.

SVENSSON, A., JOHNSSON, F. & LECKNER, B. 1996. Bottom bed regimes in a circulating fluidized bed boiler. *International Journal of Multiphase Flow,* 22**,** 1187-1204.